Can WIMP spin dependent couplings explain DAMA data, in light of null results from other experiments?

Chris Savage,[1] Paolo Gondolo,[2] and Katherine Freese[1]

[1]*Michigan Center for Theoretical Physics, Physics Department, University of Michigan, Ann Arbor, Michigan 48108, USA*
[2]*Physics Department, University of Utah, Salt Lake City, Utah 84112, USA*

(Received 20 August 2004; revised manuscript received 29 October 2004; published 8 December 2004)

We examine whether the annual modulation found by the DAMA dark matter experiment can be explained by Weakly Interacting Massive Particles (WIMPs), in light of new null results from other experiments. CDMS II has already ruled out most WIMP-nucleus spin-independent couplings as an explanation for DAMA data. Hence we here focus on spin-dependent (axial vector; SD) couplings of WIMPs to nuclei. We expand upon previous work by (i) considering the general case of coupling to both protons and neutrons and (ii) incorporating bounds from all existing experiments. We note the surprising fact that CMDS II places one of the strongest bounds on the WIMP-neutron cross section, and show that SD WIMP-neutron scattering alone is excluded. We also show that SD WIMP-proton scattering alone is allowed only for WIMP masses in the 5–13 GeV range. For the general case of coupling to both protons and neutrons, we find that, for WIMP masses above 13 GeV and below 5 GeV, there is no region of parameter space that is compatible with DAMA and all other experiments. In the range (5–13) GeV, we find acceptable regions of parameter space, including ones in which the WIMP-neutron coupling is comparable to the WIMP-proton coupling.

DOI: 10.1103/PhysRevD.70.123513 PACS numbers: 95.35.+d

I. INTRODUCTION

The dark halo of our Galaxy may consist of WIMPs (Weakly Interacting Massive Particles). Numerous collaborations worldwide have been searching for these particles. Direct detection experiments attempt to observe the nuclear recoil caused by these dark matter particles interacting with nuclei in the detectors. Indirect detection experiments search for the signatures of WIMP annihilation in the Sun, the Earth, or the Galactic Halo. It is well known that the count rate in WIMP direct detection experiments will experience an annual modulation [1,2] as a result of the motion of the Earth around the Sun: The relative velocity of the detector with respect to the WIMPs depends on the time of year.

The discovery of an annual modulation by the DAMA/NaI experiment [3] (hereafter, "DAMA") is the only positive signal seen in any dark matter search. However, recent null results from other experiments, particularly EDELWEISS and CDMS II, severely bound the parameter space of WIMPs that could possibly explain the DAMA data. In fact, if the interactions between WIMPs and nuclei are spin independent (SI), then CDMS II has ruled out DAMA (with some exceptions [4]). In this paper, we will consider the alternative of spin-dependent (SD) WIMP cross sections. We expand upon previous work by (i) considering the general case of coupling to both protons and neutrons and (ii) incorporating bounds from all existing experiments, including, in particular, the null results recently released by CDMS II and Super-Kamiokande (Super-K), which were not available to previous authors. Previously, Ullio *et al.* studied the cases of interactions with protons only or neutrons only [5] and made a comparison with experiments that had been performed at that time; they argued that some cases of mixed interactions would be ruled out as well. In 2003 Kurylov and Kamionkowski performed a general analysis for pointlike WIMPs of arbitrary spin to find what WIMPs were compatible with DAMA and the null experiments at the time [6]. Giuliani looked at the more general case of mixed interactions [7], but only applied the analysis to DAMA for a limited choice of WIMP mass. We here perform a general analysis with coupling to both protons and neutrons to see if any parameter space remains that could explain simultaneously the DAMA and CDMS data. To be complete, we will also incorporate bounds from other experiments, including Super-K (which measures indirect detection in the Sun). Notice, however, that these indirect detection limits do not apply if WIMPs do not effectively annihilate in the Sun, as, for example, if the WIMP is not its own antiparticle and there is a sufficiently strong cosmic asymmetry in the number of WIMPs and anti-WIMPs.

We find those regions of WIMP parameter space that survive all existing experiments for the case of spin-dependent interactions. Although the current CDMS data are more stringent than those studied in previous work, our final bounds are somewhat less restrictive for WIMP-proton coupling than those quoted by Ullio *et al.* because the latest results released by Super-K are less restrictive than those approximated by Ullio *et al.* and because we are reluctant to extend Super-K data beyond those published by the experimentalists (as elaborated in the discussion section at the end of the paper).

We also note that, although CDMS data have typically been ignored in the spin-dependent sector due to the

small natural abundance of spin odd isotopes in the detector, in fact CDMS II places one of the strongest bounds on the WIMP-neutron cross section (note that even CDMS I placed interesting bounds particularly at low masses).

II. WIMP DETECTION

The basic idea underlying WIMP direct detection is straightforward: The experiments seek to measure the energy deposited when a WIMP interacts with a nucleus in the detector [8].

If a WIMP of mass m scatters elastically from a nucleus of mass M, it will deposit a recoil energy $E = (\mu^2 v^2/M)(1 - \cos\theta)$, where $\mu \equiv mM/(m + M)$ is the reduced mass, v is the speed of the WIMP relative to the nucleus, and θ is the scattering angle in the center of mass frame. The differential recoil rate per unit detector mass for a WIMP mass m, typically given in units of counts/kg/day/keV, can be written as

$$\frac{dR}{dE} = \frac{\rho}{2m\mu^2}\sigma(q)\eta(E, t) \tag{1}$$

where $\rho = 0.3\ \mathrm{GeV/cm^3}$ is the standard local halo WIMP density, $q = \sqrt{2ME}$ is the nucleus recoil momentum, $\sigma(q)$ is the WIMP-nucleus cross section, and information about the WIMP velocity distribution is encoded into the mean inverse speed $\eta(E, t)$,

$$\eta(E, t) = \int_{u > v_{\min}} \frac{f_{\mathrm{d}}(\mathbf{u}, t)}{u} d^3u. \tag{2}$$

Here

$$v_{\min} = \sqrt{\frac{ME}{2\mu^2}} \tag{3}$$

represents the minimum WIMP velocity that can result in a recoil energy E and $f_{\mathrm{d}}(\mathbf{u}, t)$ is the (usually time-dependent) distribution of WIMP velocities $\mathbf{u}$ relative to the detector.

For WIMPs in the Milky Way halo, the most frequently employed WIMP velocity distribution is that of a simple isothermal sphere [1]. In such a model, the Galactic WIMP speeds with respect to the halo obey a Maxwellian distribution with a velocity dispersion σ_h truncated at the escape velocity v_{esc},

$$f_h(\mathbf{v}) = \begin{cases} \frac{1}{N_{\mathrm{esc}}\pi^{3/2}\overline{v}_0^3} e^{-\mathbf{v}^2/\overline{v}_0^2}, & \text{for } |\mathbf{v}| < v_{\mathrm{esc}} \\ 0 & \text{otherwise.} \end{cases} \tag{4}$$

Here

$$\overline{v}_0 = \sqrt{2/3}\sigma_h \tag{5}$$

and

$$N_{\mathrm{esc}} = \mathrm{erf}(z) - 2z\exp(-z^2)/\pi^{1/2}, \tag{6}$$

with $z = v_{\mathrm{esc}}/\overline{v}_0$, is a normalization factor. For the sake of illustration, we take $\sigma_h = 270$ km/s and $v_{\mathrm{esc}} = 650$ km/s. The results for the mean inverse speed $\eta(E, t)$ for the case of the isothermal sphere have previously been calculated and can be found, e.g., in [2,9].

It is well known that the count rate in WIMP detectors will experience an annual modulation [1,2] as a result of the motion of the Earth around the Sun: The relative velocity of the detector with respect to the WIMPs depends on the time of year. The disk of the galaxy rotates through the relatively stationary halo, giving the Sun a velocity $v_\odot = 232$ km/s relative to the halo. In addition, the Earth travels about the Sun at $V_\oplus = 30$ km/s (relative to the Sun), with the Sun's motion in the Galaxy being at 60° from the Earth's orbital plane ($\mathbf{v}_\oplus \equiv \mathbf{v}_\odot + \mathbf{V}_\oplus$).

We will use the isothermal halo model in our calculations, but its validity is by no means guaranteed—the actual halo may be squashed or anisotropic [10]—may contain streams from smaller galaxies in the process of being absorbed by the Milky Way [11] or may, in fact, not yet be thermalized.

An alternative way to search for WIMP dark matter of relevance to this paper is via indirect detection of WIMP annihilation in the Sun. When WIMPs pass through a large celestial body, such as the Sun or the Earth [12,13], interactions can lead to gravitational capture if enough energy is lost in the collision to fall below the escape velocity. Captured WIMPs soon fall to the body's core and eventually annihilate with other WIMPs. These annihilations lead to high-energy neutrinos that can be observed by Earth-based detectors such as Super-Kamiokande [14], Baksan [15], and AMANDA [16], and the IceCube [17] and ANTARES [18] projects. The annihilation rate depends on the capture rate of WIMPs, which is in turn determined by the WIMP scattering cross section off nuclei in the celestial body. While the Earth is predominantly composed of spinless nuclei, the Sun is mostly made of hydrogen, which has spin. Thus the spin-dependent cross section of WIMPs off nucleons can be probed by measuring the annihilation signals from WIMP annihilation in the Sun. Other indirect detection methods search for WIMPs that annihilate in the Galactic Halo or near the Galactic Center where they produce neutrinos, positrons, or antiprotons that may be seen in detectors on the Earth [19,20].

III. SPIN-INDEPENDENT CROSS SECTION

The cross section for spin-independent WIMP interactions is given by

$$\sigma_{\mathrm{SI}} = \sigma_0 F^2(q) \tag{7}$$

where σ_0 is the zero-momentum WIMP-nuclear cross section and $F(q)$ is the nuclear form factor, normalized to $F(0) = 1$; a description of these form factors may be found in [21,22]. For purely scalar interactions,

$$\sigma_{0,\mathrm{scalar}} = \frac{4\mu^2}{\pi}[Zf_p + (A - Z)f_n]^2. \quad (8)$$

Here Z is the number of protons, $A - Z$ is the number of neutrons, and f_p and f_n are the WIMP couplings to the proton and nucleon, respectively. In most instances, $f_n \sim f_p$; the WIMP-nucleus cross section can then be given in terms of the WIMP-proton cross section as a result of Eq. (8):

$$\sigma_0 = \sigma_p\left(\frac{\mu}{\mu_p}\right)^2 A^2 \quad (9)$$

where the μ_p is the proton-WIMP reduced mass, and A is the atomic mass of the target nucleus.

In this model, for a given WIMP mass, σ_p is the only free parameter and its limits are easily calculated for a given experiment. These limits are routinely calculated by the dark matter experiments and it has been found that the DAMA and CDMS results are incompatible for most WIMP mass in the spin-independent case, assuming the standard isothermal halo [23] (an exception is the case of light WIMPs of 6–9 GeV discussed in [4]).

IV. SPIN-DEPENDENT CROSS SECTION

For the remainder of the paper, we will focus on spin-dependent interactions. The generic form for the spin-dependent WIMP-nucleus cross section includes two couplings—the WIMP-proton coupling a_p and the WIMP-neutron coupling a_n,

$$\sigma_{\mathrm{SD}}(q) = \frac{32\mu^2 G_F^2}{2J+1}[a_p^2 S_{pp}(q) + a_p a_n S_{pn}(q) + a_n^2 S_{nn}(q)]. \quad (10)$$

Here the nuclear structure functions $S_{pp}(q)$, $S_{nn}(q)$, and $S_{pn}(q)$ are functions of the exchange momentum q and are specific to each nucleus. The quantities a_p and a_n are actually the axial four-fermion WIMP-nucleon couplings in units of $2\sqrt{2}G_F$ [24–26].

For a given experiment and WIMP mass, one can integrate Eq. (1) over an energy bin E_1–E_2, using the above cross section and factoring in efficiencies, quenching factors, etc., to obtain the expected number of recoil events N_{rec} as a function of the parameters a_p and a_n:

$$N_{rec}(a_p, a_n) = A_{rec}a_p^2 + B_{rec}a_p a_n + Ca_n^2. \quad (11a)$$

A_{rec}, B_{rec}, and C_{rec} are constants that can be calculated from the integration (see the appendix). They differ between experiments and they depend on the WIMP mass and WIMP velocity distribution. The expected value of the amplitude of the annual modulation can be similarly calculated as Eq. (11a):

$$N_{ma}(a_p, a_n) = A_{ma}a_p^2 + B_{ma}a_p a_n + C_{ma}a_n^2 \quad (11b)$$

where N_{ma} is the modulation amplitude and A_{ma}, B_{ma}, and C_{ma} will again be calculable strictly from the experimental parameters and the WIMP mass and velocity distribution. A more detailed discussion of calculating N_{rec}, N_{ma}, and the associated constants is given in the appendix. Null search results place an upper limit on N_{rec} ($N_{rec} < N_{rec,\max}$), which then constrains the possible values for a_p and a_n. A positive modulation signal, such as in DAMA ($N_{ma,\min} < N_{ma} < N_{ma,\max}$), likewise constrains the possible values for a_p and a_n.

Previous authors, when searching for regions compatible with both the DAMA signal and the null results of other experiments [5], have studied the following two specific cases: (i) $a_n = 0$ so that only protons contribute to WIMP interactions, and (ii) $a_p = 0$ so that only neutrons contribute. Here we examine the more general case where both a_p and a_n may be nonzero (some of this parameter space has also been examined by Giuliani [7]). To do this, we examine the form of the limits on a_p and a_n implied by Eqs. (11a) and (11b).

Equations (11a) and (11b) describe a conic section in the a_p-a_n plane. This conic section can be an ellipse, a hyperbola, or a set of two straight lines (it cannot be a parabola because linear terms in a_p or a_n are absent). Which is the case depends on the values of the coefficients A, B, and C. For the benefit of the reader, we will briefly review the relevant shapes here (our conics are always centered at the origin, so we only describe such cases below).

An ellipse in the x-y plane can be written as

$$\frac{x^2}{a^2} + \frac{y^2}{b^2} = 1. \quad (12)$$

This ellipse is symmetric about the x and y axes. Adding a cross term (i.e., xy) in Eq. (12) [like the B term in Eqs. (11a) and (11b)] essentially rotates the ellipse—the major and minor axes do not lie on the x and y axes, but along some new rotated axes.

Another conic section is the hyperbola:

$$\frac{x^2}{a^2} - \frac{y^2}{b^2} = 1 \quad (13)$$

which, in this form, gives two branches of a hyperbola open along the $+x$ and $-x$ directions. Rotation of this form also leads to a cross term.

Two parallel lines are also a conic (technically, a "degenerate" conic), that can be written in the form, e.g.,

$$x^2 = a^2 \quad (14)$$

which describes two lines parallel to the y axis, located at $x = +a$ and $x = -a$. Other parallel lines can be rotated into this form as well.

Note that, while other conics exist besides the three described, these are the only forms possible for Eqs. (11a)

and (11b) (which are not the most general second degree polynomials).

Equations (11a) and (11b) can, under suitable rotation in the a_p-a_n plane, be expressed in one of the forms in Eqs. (12), (13), or (14). The shape of our conic can be determined by the value of the discriminant

$$\gamma \equiv B^2 - 4AC \tag{15}$$

as follows: $\gamma < 0$ corresponds to an ellipse, $\gamma > 0$ to a hyperbola, and $\gamma = 0$ to two parallel lines. Because of our conics always being centered at the origin, there is a symmetry under $(a_p, a_n) \rightarrow (-a_p, -a_n)$.

Null result experiments provide an upper bound $N_{\max}$ on the number of recoils or modulation amplitude. This upper bound restricts the allowed a_p-a_n parameter space to the region inside the ellipse defined by $N_{\max}$ [for the case in which Eqs. (11a) and (11b) describe an ellipse], or to the region containing the origin between the two branches of the hyberbola or the two parallel lines defined by $N_{\max}$ [for the case in which Eqs. (11a) and (11b) describe a hyperbola or two straight lines]. Couplings outside these regions would lead to more recoils than observed; couplings within these regions yield less recoils than $N_{\max}$.

Experiments which obtain positive signals (such as claimed by DAMA) restrict the a_p-a_n parameter space to a band in the shape of the appropriate conic. The width of the band is defined by the uncertainty in the observed signal (the uncertainty and, hence, the width of the band can be given to various degrees of accuracy, e.g., 1 or 2σ). For example, if the conic is a circle, the allowed region would be an annulus; regions "outside" this annulus would give either too small or too large a signal.

The relative magnitudes of A, B, and C in Eqs. (11a) and (11b) are primarily dependent upon the structure functions of Eq. (10). At zero recoil energy, the structure functions in Eqs. (11a) and (11b) for a single nuclear element form a complete square, of the form $N \propto (\alpha a_p + \beta a_n)^2$ [see, e.g., Eq. (13) of Ref. [27]]. This is a rotation of Eq. (14). Hence for $q = 0$, we have $\gamma = 0$ and the appropriate conics are two parallel lines. However, at nonzero momentum transfer, interference and spin effects destroy the symmetry so that different conics may result. In addition, detectors with multiple elements, such as the NaI of DAMA, have structure functions from all of these elements contributing to the coefficients in Eqs. (11a) and (11b); the resulting conic may be very different to that obtained from the individual elements [see, e.g., Fig. 4 (below)]. For the experiments studied in this paper, we find that the relevant conics are either two parallel lines or ellipses. Some of the ellipses are so elongated as to appear as two parallel lines in our plots.

We will examine the allowed shapes in the a_p-a_n plane for current experiments and then determine where they overlap. In this way we will find those regions in parameter space that are consistent with all the current experimental results.

V. EXPERIMENTS

The constraints from different experiments on the a_p-a_n phase space are highly dependent on the choice of detector materials. Odd Z elements, such as sodium, iodine, and hydrogen, are more sensitive to a_p and thus generate narrow ellipses with the semiminor axis close to the a_p axis (interference effects can cause the ellipse to be rotated slightly). Conversely, elements with an odd number of neutrons, such as xenon-129, silicon-29, and germanium-73, are more sensitive to a_n and their associated ellipses have semiminor axes near the a_n axis. Spinless elements such as most isotopes of silicon and germanium (used by many experiments looking for spin-independent couplings), provide essentially no constraint for either a_p or a_n.

Table I (extended from [4]) displays the various experimental constraints used to generate our results. In Figs. 1 and 2, we show the limits from various experiments on the WIMP-proton and WIMP-neutron allowed couplings for the cases $a_n = 0$ and $a_p = 0$, respectively. Because of the novel detection technique used by SIMPLE (and the additional complexities involved) [35], we did not reanalyze their data in our study, but include in Fig. 2 the WIMP-neutron cross section presented in Fig. 1 of [7]. The full ZEPLIN I results were not available during the writing of this paper so were not included in our analysis; however, a preliminary limit presented by the ZEPLIN group is also included in Fig. 2 [36].

Several experiments providing recent results, including Elegant V (NaI), CRESST I (Al), SIMPLE (F), and DAMA/NaI, used odd Z nuclei and were thus more sensitive to the WIMP-proton coupling a_p. Other experiments, including DAMA/Xe-2 (Xe-129), CRESST II (Ca-43, W-183, and O-17), Edelweiss (Ge-73), ZEPLIN I (Xe-129 and Xe-131), and CDMS (Si-29 and Ge-73) used neutron-odd nuclei and were more sensitive to the WIMP-neutron coupling a_n. We note, however, that each of these experiments has some sensitivity to both a_p and a_n, as the minor axes of their ellipses are *not exactly aligned* with either a_p or a_n. Hence, surprisingly, CRESST and SIMPLE obtain very good results on WIMP-neutron coupling due to their low thresholds.

The only experiment to claim a result, DAMA/NaI, uses odd Z NaI detectors and a large exposure to search for an annual modulation. They observe an annual modulation amplitude of 0.0200 ± 0.0032 events/kg/day/keVee over electron-equivalent recoil energies of 2–6 keV. Such a modulation has been shown to be generally inconsistent with other experiments for spin-independent interactions, but we shall see there are choices of parameters still allowed for the spin-

TABLE I. Experimental constraints used in this study. Notes to the table: (§) recoil energy dependent efficiency of 7.6% (5 keV $< E <$ 10 keV), 22.8% (10 keV $< E <$ 20 keV), and 38% ($E >$ 20 keV); (†) upper limit assuming no detected event; (‡) limits generated based upon the binned data available in the corresponding papers (does not include any background subtraction and may be conservative); (○) from an electron-equivalent threshold of 13 keVee, using the quenching factor $Q = E_{ee}/E$ equal to 0.44 for Xe [28]; (◇) from an electron-equivalent thresholds of 2 keVee (DAMA/NaI) and 4 keVee (Elegant V), using Q equal to 0.09 for I and 0.3 for Na [3]; (●) amplitude of annual modulation.

Experiment	Exposure [kg-day]	Threshold [keV]	Efficiency [%]	Constraint (for stated recoil energies)	Reference
CDMS I	Si: 6.58	5	(§)	5–55 keV: <2.3 events (†)	[29]
CDMS II	Ge: 52.6	10	(§)	10–100 keV: <2.3 events (†)	[23]
CDMS II (projection)	Si: 300 Ge : 1200	5	(§)	5–100 keV: <2.3 events (†)	[30]
EDELWEISS	Ge: 8.2	20	100	20–100 keV: <2.3 events (†)	[31]
CRESST I	Al_2O_3: 1.51	0.6	100	(‡)	[32]
CRESST II	$CaWO_4$: 10.448	10	100	Ca + O, 15–40 keV: <6 events W, 12–40 keV: <2.3 events (†)	[33]
DAMA/Xe-2	Xe: 1763.2	30 (○)	100	(‡)	[28]
DAMA/NaI	NaI: 107 731	I: 22 (◇) Na: 6.7 (◇)	100	2–6 keVee: 0.0200 ± 0.0032/kg-day-keVee (●)	[3]
Elegant V	NaI: 111 854	I: 44 (◇) Na: 13.4 (◇)	100	4–5 keVee: 0.009 ± 0.019/kg-day-keVee (●)	[34]

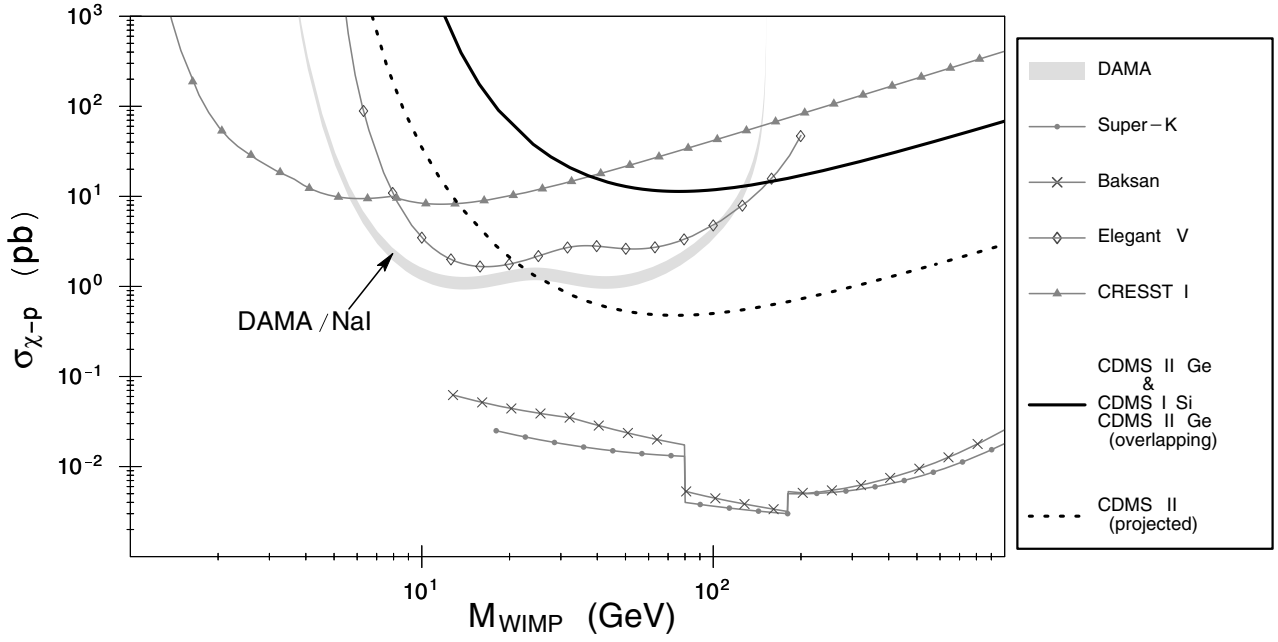

FIG. 1. WIMP-proton cross-section limits for the case $a_n = 0$. The CDMS Si + Ge limit overlaps that of Ge only; the Si is relatively insensitive in this case. Super-K only analyzed their data for WIMP masses above 18 GeV; their limit is taken from Fig. 14 of [14]. Baksan analyzed fluxes down to 13 GeV. Super-K and Baksan rule out the DAMA results over their analysis ranges and CRESST I limits DAMA at low masses, but WIMPs between 6–13 GeV are consistent with all results for this case.

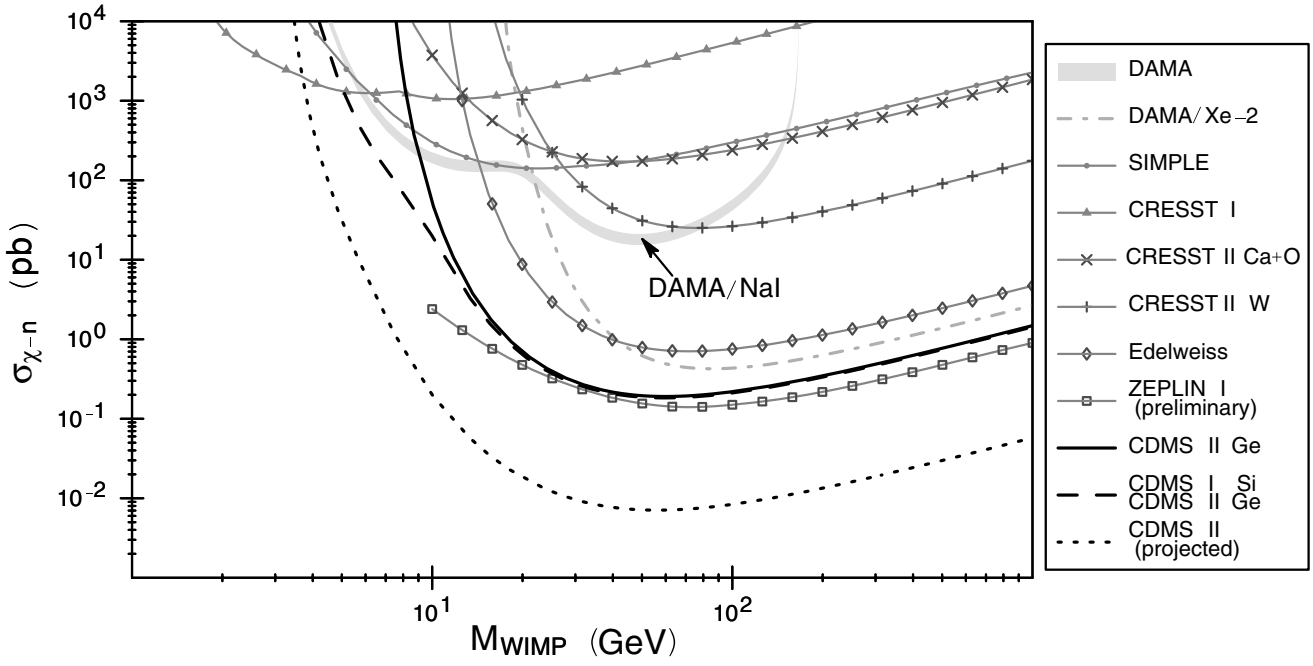

FIG. 2. WIMP-neutron cross-section limits for the case $a_p = 0$. SIMPLE limits are taken from Fig. 1 of [7]. The addition of the Si data clearly benefits CDMS at lower masses, ruling out DAMA for this simple case.

dependent case. The DAMA limits we place in a_p-a_n space are those that reproduce the above modulation amplitude, using the structure functions given by Ressell and Dean [37]. The WIMP cross sections on protons and neutrons implied by the DAMA result are plotted in Figs. 1 and 2, respectively. Kinematics alone can restrict the allowed masses of this modulation: Small masses do not generate enough recoils above threshold. One can see this in the figures as DAMA begins to lose sensitivity below about 4 GeV, requiring large cross sections to account for the observed signal. This feature is common to all dark matter experiments and lower threshold energies are required to detect the smaller recoil energies of low masses. This lower limit on sensitivity is also dependent on the parameters of the velocity distribution and may change significantly in the presence of streams [4]. Larger masses are also ruled out as the phase of the modulation would be reversed. For the 2–6 keV data plotted, the limit is roughly 180 GeV; however, this limit is dependent upon the range of recoil energies. Freese and Lewis have examined this phenomenon and determined that masses above 103 GeV would reverse the modulation at 2 keV for DAMA [38]. In addition to the 2–6 keV data, DAMA released modulation amplitudes for slightly different recoil bins, namely, for recoil energies 2–4 keV (0.0233 ± 0.0047/kg/day/keVee) and 2–5 keV (0.0210 ± 0.0038/kg/day/keVee). At the masses we are considering (< 100 GeV), the results of this paper are the same for any of the three DAMA binnings.

All other experiments have null results which place bounds on the couplings. Elegant V used NaI detectors to search for an annual modulation and found no counts above the statistically limiting background [34]. While providing one of the best exclusion limits for a proton-only coupling at low WIMP masses, the sensitivity of this experiment is not enough to examine the DAMA observed region (see Fig. 1). CRESST I [32] and SIMPLE [35] provide similar limits on WIMP-proton coupling. As mentioned above, due to their very low thresholds, CRESST I and SIMPLE also provide what have been the best neutron-only limits at low WIMP masses. DAMA/Xe-2, a neutron-odd experiment bounds the WIMP-neutron cross section above 40 GeV [28]. Our examination of Edelweiss (similar to CDMS, described below) shows that they produce a similar limit to DAMA/Xe-2 [31] (see Fig. 2).

Super-Kamiokande, on the other hand, is an indirect detection experiment, searching for high-energy neutrinos produced by the annihilation of WIMPs in the Sun's core after being gravitationally captured. Since the Sun is predominantly composed of hydrogen, the capture rate (and thus neutrino flux) is particularly sensitive to the WIMP-proton coupling a_p. The Super-K detector searched for this additional neutrino flux by observing upward moving muons (induced by muon neutrinos) [14]. The lack of an additional muon signal leads to the most significant a_p bounds above the analysis threshold WIMP mass of 18 GeV; below this mass, a significant portion of the muons would stop in the detector, rather than pass through, making the data more difficult to analyze. Discontinuities of the Super-K published limits occur at 80 GeV (W mass) and 174 GeV (top mass) due to different

possible annihilation products. The Super-K WIMP-proton cross-section limits are shown in Fig. 1; these limits are taken directly from Ref. [14], derived therein using the model-independent technique of Kamionkowski *et al.* [39]. We note that the bounds from Super-K rely on three assumptions: First, we assume that the WIMPs have achieved equilibrium in the Sun, so that the capture rate is equal to the annihilation rate; this assumption is almost certainly correct, particularly at small WIMP masses. Second, we assume that either WIMPs are equal to their antipartners so that they can annihilate among themselves or, if WIMPs are not the same as the anti-WIMPs, that there is no WIMP/anti-WIMP asymmetry. Third, the WIMPs do not decay to light fermions only (in which case fewer observable neutrinos would be produced). The second and third ways to evade the Super-K bounds were pointed out by Kurylov and Kamionkowski [6]. Here we assume that all three assumptions are correct; then Super-K rules out the proton-only coupling for WIMP masses above 18 GeV.

Baksan, another indirect detection experiment, provides the tightest bounds on proton-only coupling between 13 and 18 GeV. Although Baksan provides weaker WIMP-induced muon flux limits than Super-K above 18 GeV, the Baksan experiment has analyzed these fluxes down to a lower WIMP mass of 13 GeV [15]. These flux limits can be used to determine WIMP-proton cross-section limits in the same manner as Super-K; such an analysis is not available from the Baksan collaboration at this time. However, the Baksan cross-section limit can be determined by rescaling the Super-K limit by the relative flux limits of these two experiments (since the expected flux is proportional to this cross-section). Below 18 GeV, where there is no Super-K limit to rescale, we extrapolate the Baksan cross-section limit using their given flux limit and the WIMP mass dependence of the expected flux, given by Eq. (9.55) of Ref. [22]. We find that Baksan rules out proton-only coupling down to WIMP masses of 13 GeV.

CDMS II, in the Soudan Underground Laboratory, uses silicon and germanium detectors with strong discrimination to provide the strongest spin-independent cross-section limits to date [23]. Analysis of CDMS results in the spin-dependent sector has consistently been ignored, as the small natural abundance of spin odd isotopes in silicon (4.68% Si-29) and germanium (7.73% Ge-73) has given the impression that CDMS is not sensitive enough for any significant spin-dependent results. Our analysis, however, shows that the extremely clean, background-free data is sufficient to overcome the smaller spin sensitive mass, with the odd neutron Ge-73 (silicon data has not yet been published) providing significant limits to a_n. The limits we obtain are due to the fact that no events were observed in 52.6 days of livetime for four 0.250 kg germanium detectors over 10 to 100 keV recoil energy, using an efficiency of 0.228 for 10–20 keV and 0.38 for 20–100 keV; an efficiency of 0.076 for 5–10 keV is used to determine limits at lower thresholds. Since silicon is lighter than germanium, it will provide better limits at small WIMP masses. As the silicon data has not yet been published for the first run of CDMS II, we augment the CDMS II Ge results with the most recent CDMS I Si data [29]. The last CDMS I run used the same detector tower as now used in CDMS II, containing two 0.100 kg silicon detectors as well as the four germanium ones. However, one of these Si detectors was contaminated and not used in the data analysis. No Si events were found in the range 5–55 keV after 65.8 days of livetime, with the same efficiencies as above. While several Si events were observed above 55 keV, these are consistent with a neutron background. Even if these events were WIMP scatters, they are not consistent with a light mass. Since the Si data is being used to extend the limits at low masses (Ge data dominates at higher masses), we feel justified in ignoring the high-energy events. CDMS hopes to install a total of five towers and achieve a total exposure during the CDMS II run of 1200 kg days for Ge and 300 kg days for Si; we will use these numbers to project future limits, assuming a 5 keV threshold and null results [30]. We have used the structure functions given by Ressell *et al.* [40] for Si-29 and Dimitrov *et al.* [41] for Ge-73; a comparison of the Ge-73 functions from Ressell shows the results are relatively insensitive to the models used to derive the form factors.

VI. RESULTS

We first present results for the simple cases where the WIMP couples to only the proton or neutron. From a combination of constraints in Fig. 2, one can see that DAMA results are not compatible with limits from other experiments for the case of the WIMP coupling with neutrons only. However, one can see in Fig. 1 that DAMA still survives for the case of proton-only coupling for masses less than 18 GeV.

Figure 1 displays the current limits for the WIMP-proton cross section assuming the WIMP couples only to the proton ($a_n = 0$). CDMS does not currently constrain this coupling. The Super-K and Baksan results, however, strongly rule out the WIMP-proton coupling that would be required to explain DAMA for masses above 13 GeV. Elegant V still allows for the DAMA observed modulation at these lower masses and CRESST I provides only a lower mass limit of 6 GeV.

Figure 2 displays the WIMP-neutron cross section in the alternative case that the WIMP couples only to the neutron $a_p = 0$. DAMA/Xe-2 and Edelweiss rule out this case for masses above 20 GeV. The surprising result is that CDMS II significantly improves upon this limit, ruling out masses above 10 GeV. Furthermore, if one includes the CDMS I Si data, CDMS rules out all of the DAMA

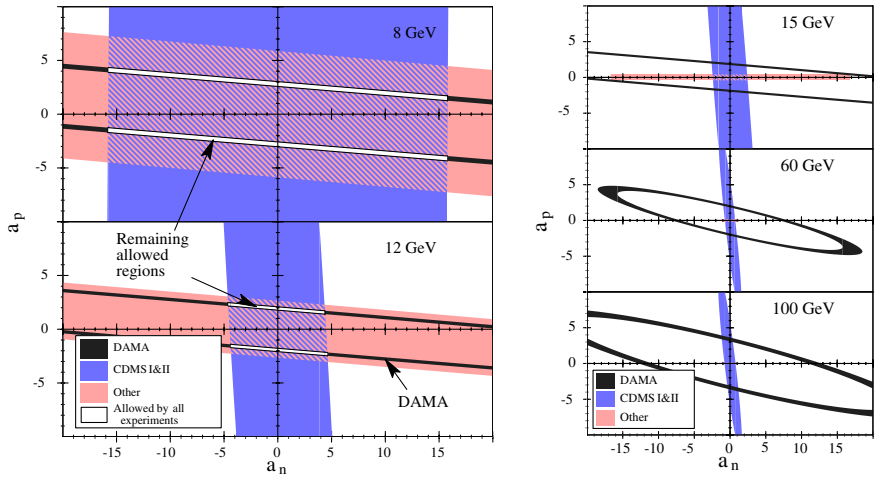

FIG. 3 (color online). Spin-dependent allowed couplings at several different WIMP masses (in different panels). The legends in the figure indicate regions allowed by different experiments. The thin black horizontal bands (ellipses at higher masses) show the region allowed by DAMA (note that the black bands are indicated as white for regions allowed by all experiments); the allowed couplings for DAMA are those that fall *on* the bands, not between them. The dark (blue) vertical regions correspond to couplings allowed by the CDMS I Si and CDMS II Ge data sets. The remaining (pink) horizontal region, labeled as other in the legend, represents couplings allowed by the combined null results of Super-K, Baksan, Elegant V, CRESST, DAMA/Xe-2, and Edelweiss (couplings outside of this region are ruled out by at least one of these experiments). The region allowed by *all* experiments is indicated by white bands. Only inside these white bands is the DAMA signal consistent with the null results from other experiments. For masses above 13 GeV there is no consistent region (no white band).

allowed region for this case. Recent ZEPLIN results are extremely powerful as well.

While the above two cases demonstrate the different sensitivities of the experiments, they are not necessarily representative of the more general parameter space, where *both* a_p and a_n may be nonzero. Figure 3 shows the a_p-a_n regions allowed by DAMA, CDMS, and a combination of the remaining experiments at several different masses for this more general case.

The DAMA observed modulation generates an elliptical ring, flattened in roughly the direction of the a_p axis (due to the odd Z NaI). (At low masses, the portion of the elliptical ring that is plotted looks like two parallel bands.) The ellipse is slightly rotated from the a_p-a_n axes; this rotation increases at larger masses as observed recoils tend to come from the iodine atoms rather than the lighter sodium (which has different structure functions). The DAMA allowed couplings are those that fall *on* the elliptical bands, not between them; couplings ''inside'' the inner edge of the elliptical ring (between the two bands of the ellipses) are too small to generate the observed modulation.

Other experiments, which have null results, place bounds on the a_p-a_n parameter space, as shown in Fig. 3. The light gray (pink) horizontal regions, labeled as ''other'' in the legend of the figure, illustrate a combination of limits from Super-K, Baksan, Elegant V, CRESST, Edelweiss, and DAMA/Xe-2 (we remind the reader that DAMA/Xe-2 is entirely different from the DAMA/NaI annual modulation results). Only couplings within these regions satisfy the null result constraints of all these experiments. Super-K and Baksan results depend upon WIMPs interacting with hydrogen, and thus inherently limit the proton coupling a_p only. The Super-K and Baksan allowed regions are bands along the a_n axis (corresponding to the region between two parallel lines). The DAMA/Xe-2 and Edelweiss allowed ellipses, whose minor axes are along the a_n direction, are far broader in the a_p direction. The intersection of these regions (horizontal Super-K and Baksan bands with vertical DAMA/Xe-2 and Edelweiss ellipses) forms a roughly rectangular region above 13 GeV, clearly visible in the 15 GeV panel and getting smaller at higher masses. Any allowed model must lie within this ''rectangle.'' Below 18 GeV, Super-K and DAMA/Xe-2 no longer provide the best limits (or any limit, in Super-K's case); below 13 GeV, Baksan and Edelweiss also lose their sensitivity. For these lower masses, Elegant V and CRESST I (included in the region labeled ''other'') provide the best limits; however, they do not significantly constrain the DAMA space between 5 and 13 GeV.

The recent CDMS results are also shown in Fig. 3. CDMS's null result, based upon odd neutron Si and Ge, generates an allowed region elongated along the a_p axis. In Fig. 3, the region allowed by the CDMS data is dark gray (blue) and is labeled ''CDMS I&II.'' The addition of CDMS I Si data increases sensitivity at low masses, due both to the lighter mass and lower threshold than the

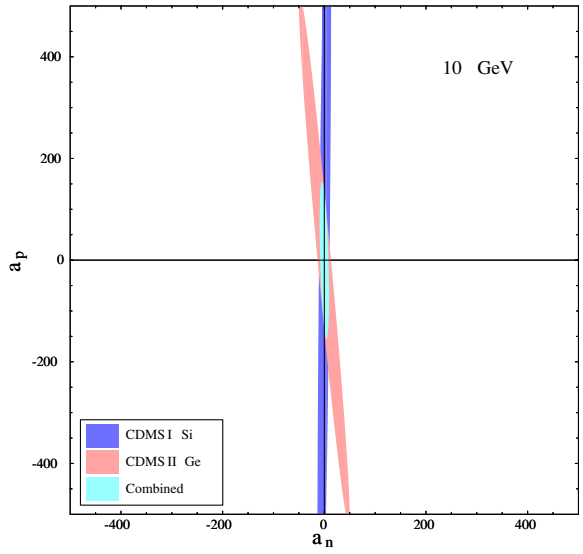

FIG. 4 (color online). Spin-dependent couplings allowed by CDMS at a WIMP mass of 10 GeV. The separate limits from Si and Ge each produce extremely long ellipses; the combined limit is significantly smaller.

CDMS II Ge data. As the sensitivity changes from predominantly Ge at high masses to Si at low masses, the shape of the allowed region rotates slightly (as Si and Ge have different structure functions).

In sum, we have applied null results from all other experiments to see whether or not DAMA annual modulation results can be compatible. The only remaining regions are shown in white bands in Fig. 3. Only WIMP masses in the range 5–13 GeV survive as spin-dependent candidates matching all the data. In the next section (SUMMARY AND DISCUSSION) we discuss the viable ranges of couplings in the a_p-a_n plane.

Note that, when one allows both a_p and a_n to be nonzero, the bounds of Figs. 1 and 2 on proton-only and neutron-only couplings can be considerably weakened. We illustrate this with an example in Fig. 4, which shows the limits in the a_p-a_n plane separately for the CDMS I Si and CDMS II Ge at a WIMP mass of 10 GeV. While Ge limits a_p to below 160 for $a_n = 0$, even a small nonzero value of a_n allows for a_p values several times larger (e.g., we can have $a_p = 330$ at $a_n = -20$). The CDMS II Ge limit in Fig. 1 for the WIMP-proton coupling applies only to the case of $a_n = 0$, but the limit in the general case is more than an order of magnitude weaker.

Referring again to Fig. 4, the Si data forms a similar elliptical limit as the Ge, but slightly rotated. Even the slight rotation is significant enough that the two narrow ellipses rarely overlap—the combined Si and Ge limit is significantly smaller than that of either of the separate limits. Detectors employing multiple elements can break the (near) degeneracy typical of individual elements.

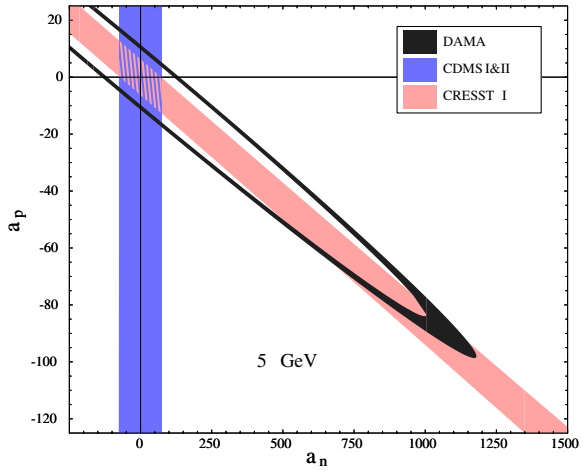

FIG. 5 (color online). Spin-dependent allowed couplings at 5 GeV for DAMA (black elliptical band), CDMS (vertical region), and CRESST I (angled region). The CDMS and CRESST I null results only allow for couplings within the intersection of their corresponding allowed regions (hatched region); this intersection does not include any couplings that can reproduce the DAMA observed modulation. Below 5 GeV, the CDMS/CRESST I constraint grows rapidly stronger relative to the DAMA required couplings. Note the axes are not at the same scale.

VII. SUMMARY AND DISCUSSION

Figure 3 illustrates our main results. When we allow both a_p and a_n to be nonzero, there is no region of parameter space with WIMP masses above 13 GeV which is compatible with both the positive results of DAMA and the null results of Super-K, DAMA/Xe-2, Edelweiss, and CDMS. Below 13 GeV, there are line segments in the a_p-a_n plane which are still compatible with the DAMA data and all null results from other experiments; CDMS II is the most constraining. At 12 GeV, the compatible line segments are $a_p = -0.084a_n + 1.94(\pm 0.16)$ with $-4.62 \leq a_n \leq 4.39$; at 8 GeV they are $a_p = -0.084a_n + 2.81(\pm 0.23)$ over $-15.8 \leq a_n \leq 15.8$ [these describe only one of the line segments, the other is found by taking $(a_n, a_p) \rightarrow (-a_n, -a_p)$]. This includes cases for which the proton and neutron couplings are comparable (e.g., $a_p = a_n = 1.8$ at 12 GeV and $a_p = a_n = 2.6$ at 8 GeV), in which case the WIMP-proton and WIMP-neutron cross sections are of the same order (equal for the given examples). We also note that only models with $|a_p| > 1$ are consistent at *any* mass. Below about 5 GeV, CRESST I becomes significant enough to exclude (in combination with CDMS) all of DAMA's parameter space (Fig. 5).

We note that the small remaining regime of spin-dependent parameter space could be confirmed or ruled out by more complete analysis of Super-K or other solar neutrino (indirect detection) data. If Super-K, Baksan, and ANTARES (or in the future IceCube and

ANTARES) were able to push down their analyses below 13 GeV WIMP masses, they would be able to either find the WIMP annihilation from the Sun compatible with DAMA, or rule out DAMA entirely as due to spin-dependent interactions of a WIMP that is its own anti-WIMP. If the WIMP and anti-WIMP abundances in the Sun would differ substantially, there would be no annihilation signal from the Sun even if WIMPs may be abundant enough to give rise to a signal in DAMA. Previously Ullio *et al.* [5] attempted to push the Super-K results down to lower WIMP masses. However, we feel that their analysis may have been too constraining due to the fact that the energy threshold for the muons in the experiments was not taken into account (it was set to zero). We feel that this analysis must be left to the experimentalists. We encourage the experimentalists to study the bounds at lower WIMP masses that would arise when one extends the analysis to more difficult cases: muons that stop in the detector, muons that start in the detector, and contained events (muons that start and stop in the detector). For the contained events one should consider both muon and electron neutrinos. If such an analysis were possible, then one could confirm or refute the remaining parameter region for spin-dependent interactions in DAMA.

In the future, as other experiments become more sensitive, they will of course further restrict the parameter space as well. New CRESST I or SIMPLE data should also be able to push down the WIMP mass compatible with DAMA. Edelweiss, CRESST II and ZEPLIN [42], whose role is similar to CDMS in this regard (their ellipses align with the a_p axis), will also become important.

Accelerator bounds on spin-dependent interactions are far weaker than the limits we have discussed from dark matter experiments. At the high energies in accelerators, the WIMPs couple directly to the quarks and can no longer be treated as effectively coupling to the nucleons as a whole. Such scattering may occur through exchange of several different particles, leading to interference effects that further reduce the cross section. Likely signatures of such scatters are also either unobservable or dwarfed by backgrounds. Looking at the case of a simple Z exchange, the lowest order case of $q\bar{q} \rightarrow Z + X$ with Z producing a WIMP pair $Z \rightarrow \chi\chi$ would not present an observable signal as the WIMP itself, being electrically neutral and weakly interacting, is not directly detectable. The signal is potentially observable if a gluon is also emitted, $q\bar{q} \rightarrow Z + g + X$, but other Standard Model processes produce the same signatures at rates much larger than those expected for a_p and a_n of order one. Even assuming no interference effects, the experimental limits from this and similar processes give $a_p \lesssim O(10^2)$, much weaker than the limits of $O(1)$ from the dark matter experiments. As a final remark, we note that the Minimal Supersymmetric extension of the Standard Model does not provide a dark matter candidate with the characteristics pointed to by our study.

ACKNOWLEDGMENTS

C. Savage thanks G. Kane and R. Schnee for useful discussions. We thank M. Kamionkowski for kind comments on the first version of this paper. We acknowledge the support of the DOE and the Michigan Center for Theoretical Physics via the University of Michigan. We thank the MCTP for hosting the Dark Side of the Universe Workshop, during which most of this work was performed.

APPENDIX: DETECTOR RECOILS

To determine the number of expected recoils for a given experiment and WIMP mass, we integrate Eq. (1) over the nucleus recoil energy to find the recoil rate R per unit detector mass:

$$R(t) = \int_{E_1/Q}^{E_2/Q} dE \epsilon(E) \frac{\rho}{2m\mu^2} \sigma(q) \eta(E, t). \tag{A1a}$$

$\epsilon(E)$ is the (energy dependent) efficiency of the experiment, due, e.g., to data cuts designed to reduce backgrounds. Q is the quenching factor relating the observed energy $E_{\rm det}$ (in some cases referred to as the electron-equivalent energy) with the actual recoil energy E_{rec}: $E_{\rm det} = QE_{\rm rec}$. The energy range between E_1 and E_2 is that of *observed* energies for some data bin of the detector (where experiments often bin observed recoils by energy). Note some single element detectors can calibrate their energy scales to $E_{\rm det} = E_{rec}$, in which case the quenching factor can be ignored. For detectors with multiple elements, the total rate is given by

$$R_{tot}(t) = \sum_i f_i R_i(t) \tag{A1b}$$

where f_i is the mass fraction and R_i is the rate [Eq. (A1a)] for element i.

The expected number of recoils observed by a detector is given by

$$N_{rec} = M_{det} T R \tag{A2}$$

where M_{det} is the detector mass and T is the exposure time. To calculate the constants in Eqs. (11a) and (11b), we first rewrite Eq. (10) as

$$\sigma_{\rm SD}(q) = h_{pp}(q) a_p^2 + h_{pn}(q) a_p a_n + h_{nn}(q) a_n^2 \tag{A3}$$

where

$$h_{ij}(q) \equiv \frac{32\mu^2 G_F^2}{2J+1} S_{ij}(q) \tag{A4}$$

is independent of the couplings a_p and a_n. The constants A_{rec}, B_{rec}, and C_{rec} in Eq. (11a) are then determined from Eq. (A2) by replacing $\sigma(q)$ in Eq. (A1a) with the appro-

priate $h_{ij}(q)$, e.g.,

$$A_{rec} = M_{det} T \int_{E_1/Q}^{E_2/Q} dE \epsilon(E) \frac{\rho}{2m\mu^2} h_{pp}(q) \eta(E, t). \quad \text{(A5)}$$

Similarly, B_{rec} is given by Eq. (A5) but with h_{pp} replaced by h_{pn}, and C_{rec} is given by Eq. (A5) but with h_{pp} replaced by h_{nn}.

For large detectors that can obtain high statistics, the annual modulation of the rate (due to the rotation of the Earth about the Sun) may be detectable, where

$$R(t) \approx R_0 + R_m \cos(\omega t). \quad \text{(A6)}$$

The rate (for most energies and for a Maxwellian velocity distribution) is maximized around June 2 and minimized around December 2; this phase is reversed at high enough energies [38]. The modulation amplitude,

$$N_{ma} \equiv R_m = \tfrac{1}{2}[R(\text{June 2}) - R(\text{Dec 2})], \quad \text{(A7)}$$

denoted by N_{ma} for consistency with Eq. (11a), can be put in the form of Eq. (11b) in the same manner as the total recoils above. Hence A_{ma} is the value of Eq. (A7) when $\sigma(q) \rightarrow h_{pp}(q)$ in Eq. (A1a):

$$A_{ma} = \int_{E_1/Q}^{E_2/Q} dE \epsilon(E) \frac{\rho}{2m\mu^2} h_{pp}(q) \frac{1}{2} [\eta(E, \text{June 2}) - \eta(E, \text{Dec 2})]. \quad \text{(A8)}$$

Similarly, B_{ma} is given by Eq. (A8) but with h_{pp} replaced by h_{pn}, and C_{ma} is given by Eq. (A8) but with h_{pp} replaced by h_{nn}.

[1] K. Freese, J. A. Frieman, and A. Gould, Phys. Rev. D **37**, 3388 (1988).
[2] A. K. Drukier, K. Freese, and D. N. Spergel, Phys. Rev. D **33**, 3495 (1986).
[3] DAMA Collaboration, R. Bernabei *et al.*, Riv. Nuovo Cimento **26N1**, 1 (2003).
[4] G. Gelmini and P. Gondolo, hep-ph/0405278.
[5] P. Ullio, M. Kamionkowski, and P. Vogel, J. High Energy Phys. 07 (2001) 044.
[6] A. Kurylov and M. Kamionkowski, Phys. Rev. D **69**, 063503 (2004).
[7] F. Giuliani, Phys. Rev. Lett. **93**, 161301 (2004).
[8] M.W. Goodman and E. Witten, Phys. Rev. D **31**, 3059 (1985).
[9] G. Gelmini and P. Gondolo, Phys. Rev. D **64**, 023504 (2001).
[10] A. M. Green, Phys. Rev. D **66**, 083003 (2002); C. J. Copi and L. M. Krauss, Phys. Rev. D **63**, 043507 (2001); N.W. Evans, C. M. Carollo, and P.T. de Zeeuw, Mon. Not. R. Astron. Soc. **318**, 1131 (2000).
[11] K. Freese, P. Gondolo, H. J. Newberg, and M. Lewis, Phys. Rev. Lett. **92**, 111301 (2004); K. Freese, P. Gondolo, and H. J. Newberg, astro-ph/0309279; D. Stiff, L. M. Widrow, and J. Frieman, Phys. Rev. D **64**, 083516 (2001); H. J. Newberg *et al.*, Astrophys. J. **569**, 245 (2002); B. Yanny *et al.*, Astrophys. J. **588**, 824 (2003); **605**, 575(E) (2004); S. R. Majewski, M. F. Skrutskie, M. D. Weinberg, and J. C. Ostheimer, astro-ph/0304198.
[12] J. Silk, K. A. Olive, and M. Srednicki, Phys. Rev. Lett. **55**, 257 (1985); K. Freese and M. Kamionkowski, Phys. Rev. D **55**, 1771 (1997).
[13] K. Freese, Phys. Lett. **167B**, 295 (1986); L. M. Krauss, M. Srednicki, and F. Wilczek, Phys. Rev. D **33**, 2079 (1986).
[14] Super-Kamiokande Collaboration, S. Desai *et al.*, Phys. Rev. D **70**, 083523 (2004).
[15] O.V. Suvorova, hep-ph/9911415; M. M. Boliev, E.V. Bugaev, A.V. Butkevich, A. E. Chudakov, O.V. Suvorova, V. N. Zakidyshev, and S. P. Mikheev, in Proceedings of the International Workshop on Aspects of Dark Matter in Astrophysics and Particle Physics, Heidelberg, Germany, 1996.
[16] AMANDA Collaboration, J. Ahrens *et al.*, Phys. Rev. D **66**, 032006 (2002).
[17] IceCube Collaboration, J. Ahrens *et al.*, Nucl. Phys. Proc. Suppl. **118**, 388 (2003).
[18] ANTARES Collaboration, F. Blanc *et al.*, presented by L. Thompson on behalf of the ANTARES Collaboration, ICRC 2003, Tsukuba, Japan, 2003.
[19] J. Silk and M. Srednicki, Phys. Rev. Lett. **53**, 624 (1984); J. R. Ellis, R. A. Flores, K. Freese, S. Ritz, D. Seckel, and J. Silk, Phys. Lett. B **214**, 403 (1988); F.W. Stecker, S. Rudaz ,and T. F. Walsh, Phys. Rev. Lett. **55**, 2622 (1985).
[20] P. Gondolo and J. Silk, Phys. Rev. Lett. **83**, 1719 (1999).
[21] P. F. Smith and J. D. Lewin, Phys. Rep. **187**, 203 (1990); J. D. Lewin and P. F. Smith, Astropart. Phys. **6**, 87 (1996).
[22] G. Jungman, M. Kamionkowski, and K. Griest, Phys. Rep. **267**, 195 (1996).
[23] CDMS Collaboration, D. S. Akerib *et al.*, Phys. Rev. Lett. **93**, 211301 (2004).
[24] P. Gondolo, hep-ph/9605290.
[25] D. R. Tovey, R. J. Gaitskell, P. Gondolo, Y. Ramachers, and L. Roszkowski, Phys. Lett. B **488**, 17 (2000).
[26] DarkSUSY.
[27] J. Engel, Phys. Lett. B **264**, 114 (1991).
[28] DAMA Collaboration, R. Bernabei *et al.*, Phys. Lett. B **436**, 379 (1998).
[29] CDMS Collaboration, D. S. Akerib *et al.*, Phys. Rev. D **68**, 082002 (2003).
[30] Correspondence with R. Schnee [CDMS Collaboration].
[31] EDELWEISS Collaboration, V. Sanglard, astro-ph/0306233.
[32] CRESST Collaboration, G. Angloher *et al.*, Astropart. Phys. **18**, 43 (2002).
[33] L. Stodolsky and F. Probst, in Proceedings of The Dark Side of the Universe, Ann Arbor, 2004.

[34] S. Yoshida *et al.*, AIP Conf. Proc. **570**, 343 (2001).
[35] SIMPLE Collaboration, J. I. Collar *et al.*, Phys. Rev. Lett. **85**, 3083 (2000).
[36] ZEPLIN I Collaboration, V. Kudryavtsev *et al.*, IDM 2004, Edinburgh, Scotland, 2004.
[37] M. T. Ressell and D. J. Dean, Phys. Rev. C **56**, 535 (1997).
[38] M. Lewis and K. Freese, Phys. Rev. D **70**, 043501 (2004).
[39] M. Kamionkowski, K. Griest, G. Jungman, and B. Sadoulet, Phys. Rev. Lett. **74**, 5174 (1995).
[40] M. T. Ressell, M. B. Aufderheide, S. D. Bloom, K. Griest, G. J. Mathews, and D. A. Resler, Phys. Rev. D **48**, 5519 (1993).
[41] V. Dimitrov, J. Engel, and S. Pittel, Phys. Rev. D **51**, 291 (1995).
[42] R. Luscher *et al.*, Nucl. Phys. Proc. Suppl. **95**, 233 (2001).